R. Soc. London, B 304, 551-565.
Harrison, P. M., Ford, G. G., Rice, R. W., Smith, J. M. A., Treffry, A., & White, J. L. (1986a) in *Frontiers in Bioinorganic Chemistry* (Xavier, A. V., Ed.) pp 268-277, VCH Verlagsgesellschaft, Weinheim.
Harrison, P. M., Treffry, A., & Lilley, T. H. (1986b) *J. Inorg. Biochem. 27*, 287-293.
Leach, B. S., May, M. E., & Fish, W. (1976) *J. Biol. Chem. 251*, 3856-3861.
Macara, I. G., Hoy, T. G., & Harrison, P. M. (1973) *Biochem. J. 135*, 785-789.
Niederer, W. (1970) *Experientia 26*, 218-220.
Pâques, E. P., Pâques, A., & Crichton, R. R. (1980) *Eur. J. Biochem. 107*, 447-453.
Rice, D. W., Ford, G. L., White, J. L., Smith, J. M. A., & Harrison, P. M. (1983) *Adv. Inorg. Biochem. 5*, 39-50.
Stefanini, S., Chiancone, E., Vecchini, P., & Antonini, E. (1975) in *Proteins of Iron Storage and Transport in Biochemistry and Medicine* (Crichton, R. R., Ed.) pp 295-302, North-Holland, Amsterdam.
Stefanini, S., Chiancone, E., Arosio, P., Finazzi-Agrò, A., & Antonini, E. (1982) *Biochemistry 21*, 2293-2299.
Stefanini, S., Chiancone, E., Antonini, E., & Finazzi-Agrò, A. (1983) *Arch. Biochem. Biophys. 222*, 430-434.
Treffry, A., & Harrison, P. M. (1984) *J. Inorg. Biochem. 21*, 9-20.
Wardeska, J. G., Viglione, B., & Chasteen, N. D. (1986) *J. Biol. Chem. 261*, 6677-6683.
Wetz, K., & Crichton, R. R. (1976) *Eur. J. Biochem. 61*, 545-550.
Yang, C. Y., Meagher, A., Huynh, B. H., Sayers, D. E., & Theil, E. (1987) *Biochemistry 26*, 497-503.

Fluorescence Lifetime and Solute Quenching Studies with the Single Tryptophan Containing Protein Parvalbumin from Codfish†

Maurice R. Eftink*,‡ and Zygmunt Wasylewski§

Department of Chemistry, University of Mississippi, University, Mississippi 38677, and Department of Biochemistry, Institute of Molecular Biology, Jagiellonian University, Krakow, Poland

Received December 3, 1987; Revised Manuscript Received July 21, 1988

ABSTRACT: The fluorescence decay of cod parvalbumin (both its Ca^{2+}-loaded and Ca^{2+}-depleted forms) is found to be a nonexponential process. The decay data can be fitted either by a double-exponential decay law or by a distribution of decay times. To try to distinguish between the double-exponential and distribution fits, we have collected frequency domain and steady-state fluorescence data as a function of temperature and concentration of the quencher acrylamide. We argue that the correct decay law (i.e., double exponential or distribution) must be consistent with all the data collected as a function of temperature and quencher concentrations. We employ a global analysis procedure to simultaneously fit multiple data sets that are linked by an Arrhenius or Stern-Volmer relationship. For the Ca^{2+}-loaded form of parvalbumin, the distribution model provides a consistent and reasonable fit for all of the frequency domain and steady-state data. The double-exponential model requires more fitting parameters, and some of these assume unreasonable values when this model is fitted to all of the data. For the Ca^{2+}-depleted form of the protein, it is not clear whether the double-exponential or distribution model is superior. For our steady-state solute quenching studies we present a novel analysis in terms of a distribution of quenching constants.

The intrinsic fluorescence of tryptophan residues in proteins provides a sensitive probe to study the conformational dynamics of the microenvironment of these residues. For a number of years it has been clear that the fluorescence of individual tryptophan residues may not be homogeneous. More often than not, the fluorescence decay of such residues is nonexponential (Grinvald & Steinberg, 1976; Beechem & Brand, 1985). Examples of single tryptophan residues where this nonexponentiality has been observed are ribonuclease T_1 (Chen et al., 1987; Eftink & Ghiron, 1987), holoazurin (Szabo et al., 1983; Petrich et al., 1987), melittin (Lakowicz et al., 1986), adrenocorticotropin (Ross et al., 1981a), nuclease (Grinvald & Steinberg, 1976; Brochon et al., 1974; Lakowicz et al., 1986), and phospholipase A_2 (Ludescher et al., 1985). Even the amino acid tryptophan, in water, displays a nonexponential decay (Beddard et al., 1980; Szabo & Rayner, 1980; Petrich et al., 1983).

The traditional practice has been to try to describe such decays in terms of the minimum number (i.e., two or three) of exponential decay time. The question then becomes one of trying to relate these various decay times to different conformational states and/or different kinetic processes. For example, the two decay times found for tryptophan in water have been interpreted in terms of emission from different rotamers (Szabo & Rayner, 1980; Petrich et al., 1983), or dual emission from the L_a and L_b bands of the excited indole ring (Rayner & Szabo, 1978), or as being a result of the $t^{1/2}$ term for diffusional quenching by side chains (Beddard et al., 1980). Likewise for proteins, analogous interpretations, involving two conformational states or excited-state reactions, have been offered (Beechem & Brand, 1985).

† This research was supported by National Science Foundation Grant DMB 85-11569.
‡ University of Mississippi.
§ Jagiellonian University.

0006-2960/89/0428-0382$01.50/0

Recently, it has been independently pointed out by different groups (Albery et al., 1985; James & Ware, 1985; James et al., 1985; Alcala et al., 1987a–c) that it may be more appropriate in some cases to interpret nonexponential fluorescence decays in terms of a continuous distribution of decay times. Alcala et al. (1987b,c) and Lakowicz et al. (1987a) have analyzed the fluorescence of a few single tryptophan containing proteins in terms of a distribution. Elsewhere, we have compared double-exponential and distribution fits for ribonuclease T_1 (Eftink & Ghiron, 1987).

In this paper we present frequency domain and solute quenching data for the single tryptophan containing (Trp-109), calcium binding, parvalbumin from codfish, with the goal of trying to determine whether a fit in terms of discrete fluorescence lifetimes or a distribution of lifetimes provides the best description of the data. We have studied both the Ca^{2+}-loaded and Ca^{2+}-depleted forms of parvalbumin. The fluorescence of this protein (or the homologous whiting protein, which contains a single Trp-102) has been previously studied (Permyakov et al., 1980, 1985; Eftink & Hagaman, 1985; Francois et al., 1987; Castelli et al., 1988). Permyakov et al. (1985) reported the fluorescence decay of Ca^{2+}-loaded whiting parvalbumin to be a double exponential, with $\tau_1 = 3.5$ ns, $\tau_2 = 1.4$ ns, and $f_1 = 0.7$ at 20 °C at pH 8.0. Very recently, Castelli et al. (1988) have reported a monoexponential decay, with $\tau = 4.6$ ns, for the whiting holoprotein at pH 9.0. Here we present additional frequency domain lifetime measurements, as a function of temperature and added solute quencher, for both the Ca^{2+}-loaded and Ca^{2+}-depleted states of the parvalbumin from codfish. We compare double-exponential and continuous-distribution lifetime fits. We present analyses of multiple data sets (global analyses) using a program that has recently been developed by Beechem et al. (1988). Also we present steady-state solute quenching data and a novel fit of a distribution of Stern-Volmer quenching constants to the data.

Experimental Procedures

Materials. Cod parvalbumin isotype III was isolated as described by Horrocks and Collier (1981), with the following modification. Instead of the final anion-exchange chromatographic step, the protein sample was applied to a 1.5 × 90 cm Sephadex G-75 column. The resulting protein sample showed a single band on SDS gel electrophoresis and was estimated to be >95% homogeneous by this method [although likely to still contain some isotype II, which has neither tryptophan nor tyrosine residues and thus will not interfere with fluorescence studies (Closset & Gerday, 1976)].

Acrylamide was recrystallized from ethyl acetate. Water was distilled and deionized. Other buffer components were of reagent grade.

Lifetime Measurements. Multifrequency phase/modulation fluorometry was performed with a SLM 4800 fluorometer, equipped with an update package from ISS, Inc. This instrument, the lifetime measurement procedure, and the phase-resolved spectra (PRS) measurements are described elsewhere (Eftink & Ghiron, 1987; Eftink et al., 1987). The cell holder was temperature regulated, and temperatures reported are those in the fluorescence cell. An interference filter (10-nm bandwidth) centered at 290 nm was used for excitation, and the emission was observed through a Corning 7/60 filter. For PRS measurements, an emission monochromater (16-nm slits) was used. A nonlinear least-squares fitting program (ISS, Inc.) was used to analyze the raw-phase and modulation data in terms of single-exponential and double-exponential decays (Gratton et al., 1984; Lakowicz et al., 1984). The program GLOBAL, kindly provided to us by Dr. J. Beechem, was used to perform distribution fits and simultaneous nonlinear least-squares fits on multiple, linked data sets (Beechem & Gratton, 1988; Beechem et al., 1988).

Quenching Studies. Both lifetime and intensity solute quenching studies were performed on the above phase fluorometer. A magnetic stirrer was used for mixing aliquots of a concentrated quencher solution into the cell. For the intensity studies, an excitation wavelength of 295 nm was used, and corrections were made for absorptive screening by acrylamide (Eftink & Ghiron, 1976).

The intensity quenching data were analyzed by aid of a program which we will describe elsewhere. This program calculates a nonlinear least-squares fit of the following form of the Stern–Volmer equation (Stryjewski & Wasylewski, 1986):

$$\frac{F}{F_0} = \sum_{i=1}^{n=1\text{or}2} \frac{f_i}{(1 + K_i[Q])\exp(V_i[Q])} \tag{1}$$

where F and F_0 are the fluorescence intensities in the presence and absence of quencher, Q. K_i and V_i are the dynamic ($K_i = k_{q,i}\tau_{0,i}$) and static quenching constants for component i, and f_i (where $i = 1$ and possibly 2) is the fractional intensity of a quenchable fraction. A nonlinear least-squares fit of eq 1 was performed with an IBM-type personal computer.

Distribution of Quenching Constants. In some cases the data were also analyzed in terms of a model for a distribution of quenching constants. We have written a nonlinear least-squares program to fit the following "quenching constant distribution" model to steady-state quenching data. We consider a Lorentzian distribution of K_i values (actually 18 equally spaced K_i values). The fractional intensity associated with each K_i is given as

$$f_{di} = \frac{1/[(\Delta/2)^2 + (K_i - \bar{K})^2]}{\sum_{i=1}^{18} 1/[(\Delta/2)^2 + (K_i - \bar{K})^2]} \tag{2}$$

where $\bar{K}$ is the mean K_i value, and Δ is the full width at half-maximum (FWHM) of the distribution. The resulting Stern–Volmer equation is the sum of all the K_i values, as follows:

$$\frac{F}{F_0} = \sum_{i=1}^{18} \frac{f_{di}}{(1 + K_i[Q])\exp(V[Q])} \tag{3}$$

Here we have assumed that the static quenching constant V is the same for each of the microstates in the distribution. This assumption is reasonable if the basis of the distribution of K_i values is the existence of a distribution of lifetimes. If a distribution of conformational microstates exists in which the tryptophan residue experiences a range of solvent exposure, it may also be best to express a distribution of V values, instead of a single value. As an initial assumption, we have fitted the above model with a discrete V value.

Results

Interconversion of Calcium-Loaded and Calcium-Depleted Forms. Figure 1 shows the dependence of the fluorescence intensity and λ_{max} of cod parvalbumin on the amount of EDTA added. A large red shift and slight drop in intensity are seen upon the removal of Ca^{2+} from the protein. These results are similar to those obtained by Permyakov et al. (1980) for whiting parvalbumin. In the following studies, Ca^{2+}-loaded cod parvalbumin will refer to studies in the presence of 10 mM $CaCl_2$. Ca^{2+}-depleted protein will refer to studies in the presence of 10 mM EDTA.

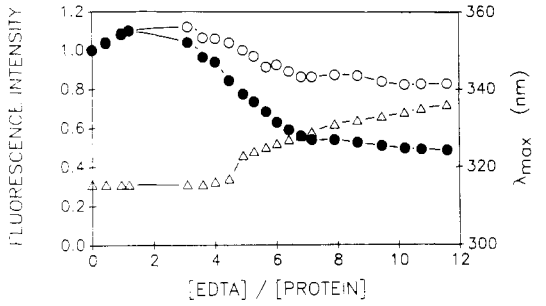

FIGURE 1: Effect of addition of EDTA on the fluorescence maximum intensity (●) and relative (integrated) intensity (○) and λ_{max} (△, right axis) of cod parvalbumin. Data obtained at 25 °C in 0.05 M Tris-HCl buffer, pH 8.0. Total protein concentration was approximately 3×10^{-5} M.

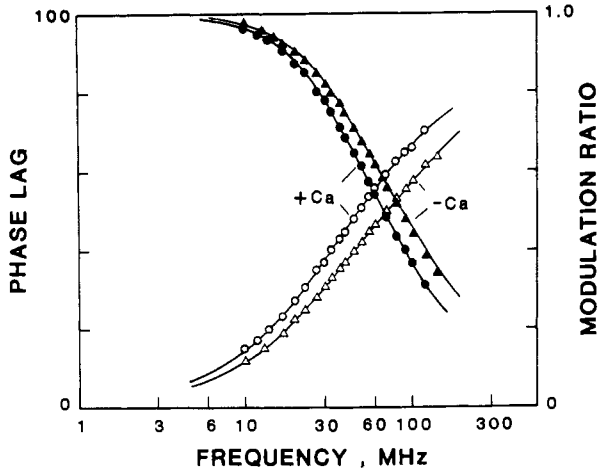

FIGURE 2: Phase and modulation measurements for Ca^{2+}-loaded (○, ●) and Ca^{2+}-depleted (△, ▲) cod parvalbumin. Temperature, 25 °C; pH 8.0; 0.05 M Tris-HCl buffer. The solid lines are two-component fits, as given in Tables I and II.

Quantitative studies by others have shown there to be two high-affinity ($K_{assoc} \approx 10^8$ M^{-1}) Ca^{2+} sites on homologous parvalbumins (Kretsinger, 1980). Scatchard plots of Ca^{2+} binding show no indication of weaker binding sites (Ogawa & Tanokura, 1986), and circular dichroism and fluorescence (of dansyl-labeled carp parvalbumin) titrations show no induced changes in the Ca^{2+} concentration range of micromolar to millimolar (Iio & Hoshihara, 1984). Although we routinely added 10 mM $CaCl_2$ to assure saturation of the protein, we have observed fluorescence lifetime and spectral data for the holoprotein (without added Ca^{2+}) to be essentially the same as that for the Ca^{2+}-loaded samples.

We used an excess of EDTA (10 mM), to form the Ca^{2+}-depleted protein, to avoid problems of incomplete removal of Ca^{2+} (Blum et al., 1977). It is possible that there is some weak binding of EDTA to the protein. For example, Haiech et al. (1979) reported a dissociation constant of 35 mM for EGTA and a homologous parvalbumin. This could potentially be a source of heterogeneity in the fluorescence of the Ca^{2+}-depleted proteins, but a much more likely source of heterogeneity stems from the fact that the protein shows a thermal transition near 32 °C when Ca^{2+} is removed (Filimonov et al., 1978). Also we note that, at 25 °C, we find no difference in the emission spectrum of the protein between 1 and 10 mM EDTA.

Fluorescence Lifetime Measurements. Typical multifrequency phase/modulation measurements for Ca^{2+}-loaded and Ca^{2+}-depleted cod parvalbumin are shown in Figure 2. In each case, a single exponential fit is unsatisfactory. A double-exponential decay law adequately described the patterns.

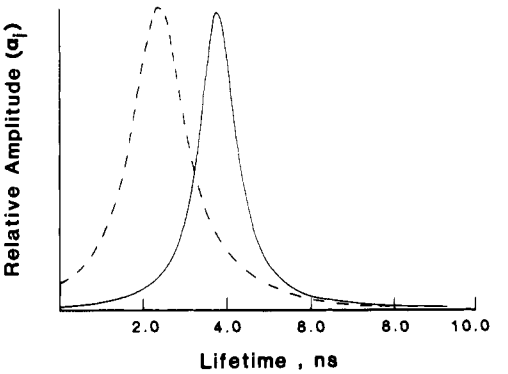

FIGURE 3: Lorentzian distribution fit for Ca^{2+}-loaded (solid curve) and Ca^{2+}-depleted (dashed curve) cod parvalbumin at 25 °C.

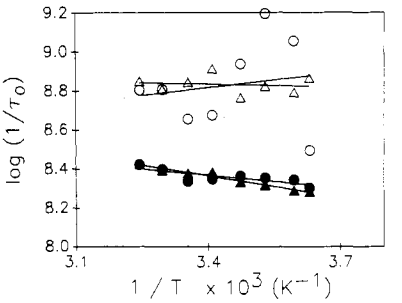

FIGURE 4: Arrhenius plot for the short (τ_1) and long (τ_2) lifetimes for parvalbumin: Ca^{2+} loaded (○, ●); Ca^{2+} depleted (△, ▲).

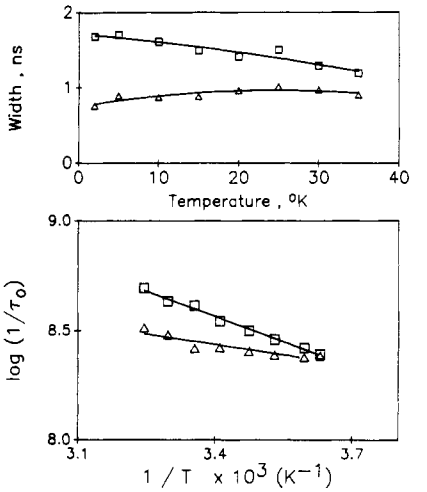

FIGURE 5: (Bottom) Arrhenius plot for the mean lifetime of the Lorentzian distribution fits: Ca^{2+} loaded (△); Ca^{2+} depleted (□). (Top) Temperature dependence of the width of the distributions (same symbols as the bottom).

We have performed such phase/modulation studies as a function of temperature, from 2 to 35 °C. In Tables I and II we list the fitting parameters for the two forms.

We have also fitted these data to a Lorentzian distribution of decay times using the program GLOBAL (Beechem et al., 1988). Figure 3 shows such a distribution fit for the Ca^{2+}-loaded (left) and Ca^{2+}-depleted (right) protein forms. The full-width half-maximum of the distribution for the latter is about twice that of the former. The reduced χ^2 for the distribution fits are nearly the same as those for the two-component fit, and as we have found for ribonuclease T_1 (Eftink & Ghiron, 1987), the error vs frequency pattern shows no systematic differences for the two fits.

Figures 4 and 5 show Arrhenius plots of the fluorescence lifetime data. Figure 4 corresponds to the two-component model. It shows much scatter for the shorter lifetime and an

Table I: Lifetime Analyses for Calcium-Loaded Parvalbumin[a]

	single-component fit		two-component fit				Lorentzian distribution fit		
temp (°C)	τ_1 (ns)	χ^2	τ_1 (ns)	τ_2 (ns)	α_1 (f_1)	χ^2	center (ns)	width (ns)	χ^2
2	4.28	2.99	5.00	3.22	0.533 (0.64)	1.12	4.15	0.71	1.25
5	4.37	5.41	4.54	0.88	0.842 (0.965)	1.13	4.18	0.89	2.04
10	4.28	5.22	4.43	0.64	0.824 (0.97)	1.00	4.09	0.87	1.88
15	4.20	5.92	4.35	1.16	0.840 (0.95)	1.29	3.93	0.88	1.68
20	4.04	5.79	4.49	2.12	0.723 (0.84)	0.68	3.78	0.96	0.81
25	4.08	5.94	4.61	2.22	0.704 (0.83)	0.52	3.81	1.01	0.56
30	3.61	9.27	4.01	1.56	0.715 (0.86)	1.67	3.30	0.97	2.18
35	3.35	11.00	3.78	1.57	0.694 (0.845)	2.77	3.07	0.90	3.41

global fit	τ_1 (ns)	τ_2 (ns)	α_1	χ^2	center (ns)	width (ns)	χ^2
α_i varied	5.34 ($E_{a,1}$ = 1.80 kcal/mol) ($E_{a,2}$ = 2.55 kcal/mol)	2.98	0.426, 0.130 0.204, 0.255 0.309, 0.023 0.312, 0.291	2.05			
α_i linked	4.66 ($E_{a,1}$ = 1.79 kcal/mol) ($E_{a,2}$ = 2.38 kcal/mol)	2.48	0.486	14.61			
Lorentzian					3.58 (E_a = 1.50 kcal/mol)	1.26	9.61

[a] Conditions: 0.05 M Tris-HCl buffer, pH 8.0, with 10 mM $CaCl_2$. The χ^2 are calculated with the following standard deviations for the phase and modulation values: σ_p = 0.5 and σ_m = 0.005. For the two-component fits, the preexponential α_1 for component 1 are given; in parentheses the fractional intensity $f_1 = \alpha_1\tau_1/\sum\alpha_i\tau_i$ of component 1 are given. For the global fits, only the α_1 are given.

Table II: Lifetime Analyses for Calcium-Depleted Parvalbumin[a]

	single-component fit		two-component fit				Lorentzian distribution fit		
temp (°C)	τ_1 (ns)	χ^2	τ_1 (ns)	τ_2 (ns)	α_1 (f_1)	χ^2	center (ns)	width (ns)	χ^2
2.0	4.68	21.27	5.24	1.37	0.697 (0.898)	0.75	4.05	1.68	3.41
5.0	4.45	25.28	5.15	1.62	0.653 (0.857)	0.82	3.78	1.70	3.11
10.0	4.14	27.31	4.84	1.51	0.625 (0.843)	0.95	3.47	1.61	3.30
15.0	3.81	26.52	4.66	1.72	0.560 (0.775)	1.40	3.17	1.49	2.98
20.0	3.50	29.29	4.14	1.22	0.587 (0.828)	1.00	2.86	1.41	3.62
25.0	3.18	42.52	4.21	1.43	0.468 (0.720)	1.29	2.43	1.50	2.58
30.0	2.97	32.97	4.06	1.56	0.408 (0.641)	2.11	2.32	1.29	2.60
35.0	2.67	33.73	3.76	1.41	0.371 (0.609)	1.82	2.02	1.19	2.11

global fit	τ_1 (ns)	τ_2 (ns)	α_1	χ^2	center (ns)	width (ns)	χ^2
α_i varied	4.05 ($E_{a,1}$ = 2.15 kcal/mol) ($E_{a,2}$ = 1.53 kcal/mol)	1.33	0.527, 0.664 0.649, 0.630 0.602, 0.563 0.495, 0.431	1.36			
α_i linked	3.96 ($E_{a,1}$ = 1.95 kcal/mol) ($E_{a,2}$ = 1.37 kcal/mol)	1.15	0.607	12.26			
Lorentzian					2.92 (E_a = 1.56 kcal/mol)	1.70	20.39

[a] Conditions: 0.05 M Tris-HCl buffer, pH 8.0, with 10 mM EDTA. See Table I for additional information.

Arrhenius activation energy, E_a, of about 2.0 kcal/mol for the longer lifetime component, for both the Ca^{2+}-loaded and Ca^{2+}-depleted forms. Figure 5 corresponds to the distribution model. It shows an E_a value of 2.0 kcal/mol for the mean lifetime for the Ca^{2+}-loaded protein and an E_a value of 3.0 kcal/mol for the Ca^{2+}-depleted protein. The top portion of Figure 4 shows that the width of the distribution varies very little with temperature for either form. The width may increase slightly with temperature for the Ca^{2+}-loaded protein and may decrease slightly with temperature for the Ca^{2+}-depleted protein.

Global nonlinear least-squares analyses of these temperature dependence data will be presented below.

Phase-Resolved Spectra. Using the two-component lifetimes in Table I, we obtained the PRS spectra shown in Figure 6 (Gratton & Jameson, 1985; Eftink et al., 1987). For the Ca^{2+}-loaded protein, the spectrum of the minor (short lifetime) component is difficult to resolve due to its small contribution, but it appears to be bluer than the major component. For the Ca^{2+}-depleted protein, the two components are easily resolved.

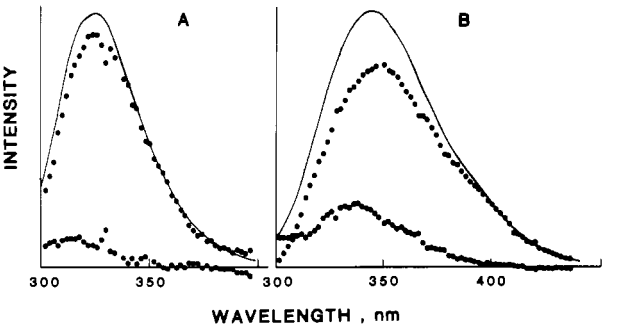

FIGURE 6: Phase-resolved spectra for Ca^{2+}-loaded (left) and Ca^{2+}-depleted (right) parvalbumin. The top spectrum is the total intensity. The subspectra correspond to that for the short and long lifetimes at 25 °C (see Tables I and II).

Table III: Lifetime Analysis for the Acrylamide Quenching of Cod Parvalbumin (Ca^{2+} Loaded)[a]

	two-component fit				distribution fit		
[acrylamide] (M)	τ_1 (ns)	τ_2 (ns)	α_1 (f_1)	χ^2	center (ns)	width (ns)	χ^2
0.0	4.60	2.22	0.704 (0.830)	0.53	3.81	1.01	0.56
0.20	4.18	1.56	0.634 (0.822)	1.83	3.13	1.21	2.81
0.46	3.72	1.47	0.499 (0.716)	2.69	2.42	1.15	3.60
0.744	3.03	1.22	0.598 (0.787)	1.59	2.23	0.84	2.41
1.06	2.72	1.17	0.519 (0.715)	2.83	1.87	0.77	3.30
1.36	2.29	0.81	0.538 (0.767)	4.05	1.52	0.74	4.99
global fit	τ_1 (ns)	τ_2 (ns)	α_1	χ^2	center (ns)	width (ns)	χ^2
α_i varied	4.47 ($k_{q,1} = 0.13 \times 10^9$ M^{-1} s^{-1})	1.53 ($k_{q,2} = 0.22 \times 10^9$ M^{-1} s^{-1})	0.772, 0.701 0.575, 0.565 0.508, 0.433	2.43			
α_i linked	4.30 ($k_{q,1} = 0.17 \times 10^9$ M^{-1} s^{-1})	0.33 ($k_{q,2} = -1.07 \times 10^9$ M^{-1} s^{-1})	0.646	4.20			
Lorentzian					3.40 ($k_q = 0.180 \times 10^9$ M^{-1} s^{-1})	1.71	8.31

[a] See Table I for information. Temperature = 25 °C.

Table IV: Lifetime Analysis for the Acrylamide Quenching of Calcium-Depleted Cod Parvalbumin[a]

	two-component fit				distribution fit		
[acrylamide] (M)	τ_1 (ns)	τ_2 (ns)	α_1 (f_1)	χ^2	center (ns)	width (ns)	χ^2
0	4.21	1.43	0.468 (0.720)	1.29	2.43	1.50	2.58
0.01	3.77	1.14	0.505 (0.770)	2.42	2.21	1.44	4.63
0.02	3.66	1.20	0.481 (0.738)	2.07	2.11	1.35	3.57
0.04	3.45	1.11	0.471 (0.729)	1.33	1.93	1.21	3.74
0.06	3.32	1.06	0.420 (0.694)	2.88	1.72	1.23	4.47
0.08	3.36	1.18	0.350 (0.604)	2.09	1.63	1.15	2.78
0.12	3.55	1.12	0.234 (0.491)	2.48	1.27	1.13	3.01
0.16	3.34	1.00	0.229 (0.501)	9.00	1.10	1.10	8.61
global fit	τ_1 (ns)	τ_2 (ns)	α_1	χ^2	center (ns)	width (ns)	χ^2
α_i varied	3.98 ($k_{q,1} = 0.43 \times 10^9$ M^{-1} s^{-1})	1.42 ($k_{q,2} = 1.90 \times 10^9$ M^{-1} s^{-1})	0.573, 0.463 0.428, 0.369 0.346, 0.321 0.274, 0.263	3.35			
α_i linked	4.56 ($k_{q,1} = 0.94 \times 10^9$ M^{-1} s^{-1})	1.84 ($k_{q,2} = 4.48 \times 10^9$ M^{-1} s^{-1})	0.345	4.28			
Lorentzian					1.94 ($k_q = 0.969 \times 10^9$ M^{-1} s^{-1})	1.77	10.77

[a] See Table II for information. Temperature = 25 °C.

Again the short-lifetime component fluoresces to the blue (λ_{max} = 320 nm) of the long-lifetime component (λ_{max} = 340 nm).

Acrylamide Quenching Lifetime Studies. Multifrequency phase/modulation data were also obtained as a function of the concentration of the quencher, acrylamide. Tables III and IV give the one-component, two-component, and distribution fits for the data for each protein form. Again, the monoexponential fit is unsatisfactory at all quencher concentrations; the double-exponential and distributions fits are similar in χ^2.

Figure 7 shows Stern–Volmer plots for the short- and long-lifetime components of the double-exponential fit and the mean lifetime of distribution fit. For the Ca^{2+}-loaded protein (top), the Stern–Volmer plots are reasonably linear for both the short- and long-lifetime components. From the best slopes and the discrete lifetimes in the absence of quencher, quenching rate constants of 0.46×10^9 M^{-1} s^{-1} and 0.15×10^9 M^{-1} s^{-1} are calculated. From the mean distribution lifetime we obtain $k_q = 0.21 \times 10^9$ M^{-1} s^{-1}. For the Ca^{2+}-depleted proteins, however, the Stern–Volmer plots have an unreasonable appearance for both the short- and long-lifetime components. The mean distribution lifetime, however, gives a linear Stern–Volmer plot with $k_q = 2.0 \times 10^9$ M^{-1} s^{-1}. The reason for the nonlinear plots for the short- and long-lifetime components is that the preexponential factor, α, for each component (see Tables III and IV) changes with acrylamide concentration in a manner inconsistent with independent dynamic quenching of each component. If the two components were independent, one would expect their preexponential factors to be constant; this is not the case for the data for either Ca^{2+}-loaded or Ca^{2+}-depleted parvalbumin.

Global Analyses. The multiple phase/modulation data sets, obtained as a function of temperature and quencher concentration, were analyzed in a global manner in order to further compare the two-component and Lorentzian distribution models. The strategy for performing such global analyses has been given by others (Beechem et al., 1983, 1988; Beechem & Gratton, 1988).

The temperature dependence data sets were linked together to have a common activation energy, E_a, and Arrhenius factor, A, for the various components. For two-component fits, the global analysis was performed either (1) by allowing the preexponential α_i values to be free floating for each temperature or (2) by fixing the α_i values to be common (or linked) for each temperature. In the former case, a very large number of fitting parameters exist (i.e., 12 for the data in Table I), as compared to the case in which the α_i are linked (i.e., 5 fitting

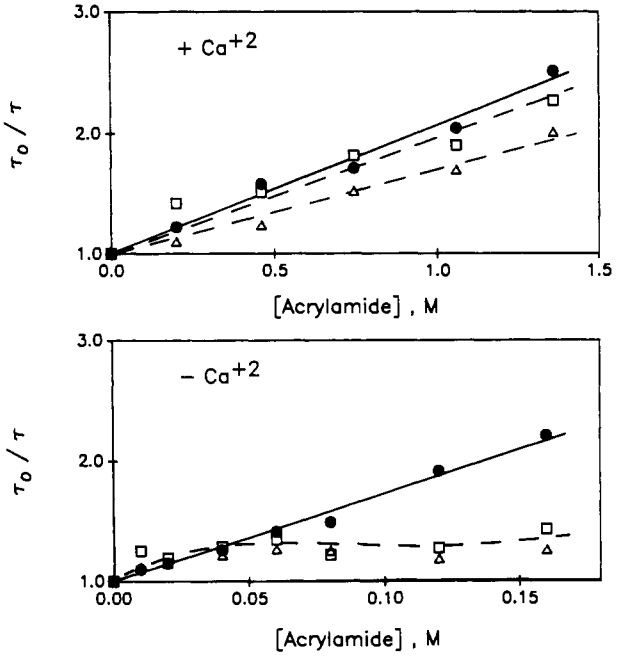

FIGURE 7: Stern–Volmer plots for the short (□) and long (△) lifetimes (double-exponential fit) and the mean (●) lifetime (distribution fit) for parvalbumin. Acrylamide was used as quencher. (Top) Ca^{2+}-loaded protein; (bottom) Ca^{2+}-depleted protein.

parameters in Table I). Consequently, better fits can be obtained when the α_i are allowed to float, but one must judge whether or not the α_i assume reasonable values.

The results of both two-component global fits are given in Table I and II for the temperature dependence of the two forms of the protein. In these tables the lifetime at 25 °C is given (instead of the Arrhenius A), along with the linked E_a and the nonlinked or linked α_i values. Below we will discuss the resonableness of the fits, but with either constraint, E_a values in the range of 2 kcal/mol are found for both the short- and long-lifetime components for both protein forms.

Global analyses of the acrylamide quenching data were also performed for the two forms of the protein. The phase/modulation data at various [Q] were linked by their unquenched lifetime, τ_{oi}, and the Stern–Volmer relationship $1/\tau_i = 1/\tau_{oi} + k_q[Q]$, where τ_i is the component lifetime in the presence of quencher and k_q is the quenching rate constant. Again, a two-component analysis was performed with the α_i forced to have a common value (10 fitting parameters in the former case; 5 fitting parameters in the latter). Given in Tables III and IV are the resulting parameters for the two-component fits. As expected, a lower χ^2 results when α_i is varied, but one should note that the fitted α_1 values are found to decrease with increasing [Q]. For this to occur, a selective, static quenching of the long-lifetime component must occur. Ordinarily one would expect the α_i to be independent of [Q]. When the α_i are linked, we find an unrealistic fit (i.e., a negative k_q value) for the Ca^{2+}-loaded protein.

Global fits of the quenching data to Lorentzian lifetime distributions were also performed. In this case, only three fitting parameters are required. Figure 8 shows the simultaneous fit to some of the quenching data for the Ca^{2+}-loaded protein. The fits to the individual data sets are certainly not optimal. However, it must be realized that satisfactory fits for six independent data sets are achieved with only three fitting parameters. The χ^2 for the global Lorentzian fit is only a factor of 3.5 times larger than that for the two-component/α_i-varied (10 parameter) fit. Thus, we find the global Lorentzian fit to the quenching data to be favored, at least

Table V: Steady-State Acrylamide Quenching of the Fluorescence Calcium-Loaded Parvalbumin[a]

discrete fit type	K_1 (M^{-1})	V_1 (M^{-1})	f_1	K_2 (M^{-1})	V_2 (M^{-1})	χ^2
I	0.620		(1.0)			0.712
II	0.505	0.086	(1.0)			0.839
III	0.586		0.986	44.3		0.465
IV	0.339	0.171	0.975	48.1	1.19	0.195

Lorentzian Distribution Fit			
$\bar{K}$ (M^{-1})	width (M^{-1})	V (M^{-1})	χ^2
0.421	0.628	0.12	0.817

[a] See Table I for conditions. Temperature = 25 °C; excitation at 295 nm; emission observed through a cutoff filter centered at 350 nm. χ^2 are based on a standard deviation of 1% for the measured fluorescence values.

Table VI: Steady-State Acrylamide Quenching of the Fluorescence Calcium-Depleted Parvalbumin[a]

discrete fit type	K_1 (M^{-1})	V_1 (M^{-1})	f_1	K_2 (M^{-1})	V_2 (M^{-1})	χ^2
I	0.61		(1.0)			5.72
II	4.89	0.617	(1.0)			0.590
III	4.55		0.248	7.09		7.11
IV	2.05	0.498	0.284	5.66	1.18	0.540

[a] Conditions given in Table II. Temperature = 25 °C; excitation at 295 nm; emission observed through a monochromater at 335 nm.

for the Ca^{2+}-loaded protein. (As will be mentioned under Discussion, we have not included a Smoluchowski transient term in our analysis. If this were included, the fit to the unimodal Lorentzian model is likely to be further improved.)

For the global distribution fit, the central lifetime and width given in Tables III and IV are for the unquenched protein. As shown by James et al. (1985), the addition of quencher will preferentially quench the longer lifetime side of a distribution, and thus the shape of the distribution will become skewed as quencher concentration increases. It is worth noting that the central, unquenched lifetime (3.4 ns) that is found in this global Lorentzian fit for the Ca^{2+}-loaded protein is in good agreement with the same parameter that is found by global analysis of the temperature dependence data (3.58 ns; see Table I). Also the k_q value (0.18×10^9 M^{-1} s^{-1}) obtained in the global Lorentzian fit is in good agreement with that determined from the nonglobal, graphical analysis in Figure 7 ($k_q = 0.21 \times 10^9$ M^{-1} s^{-1}).

For the Ca^{2+}-depleted protein, there is less agreement between the global fits to the temperature dependence and acrylamide quenching data.

In Tables I–IV we report global analyses in terms of a Lorentzian distribution of lifetimes. We have also performed global analyses (and analyses of the individual data sets) in terms of a Gaussian distribution of lifetimes. There is very little difference between the χ^2 for the fits to these two distribution shapes. The Gaussian fits tend to yield slightly broader distributions that are centered at lower lifetimes.

Acrylamide Quenching Intensity Studies. Steady-state fluorescence quenching studies were also performed. Figure 9 shows Stern–Volmer plots for the two protein forms. A larger slope and static quenching (upward curvature) is seen for the Ca^{2+}-depleted form. The plot for the Ca^{2+}-loaded protein is nearly a straight line. Tables V and VI give the best fits to the data for the Stern–Volmer equation (eq 1). Fitting parameters are shown for cases in which (I) there is only dynamic quenching of a single component, (II) there is both dynamic and static quenching of a single component, (III) there is only dynamic quenching of two components, and (IV) there is both dynamic and static quenching of two components.

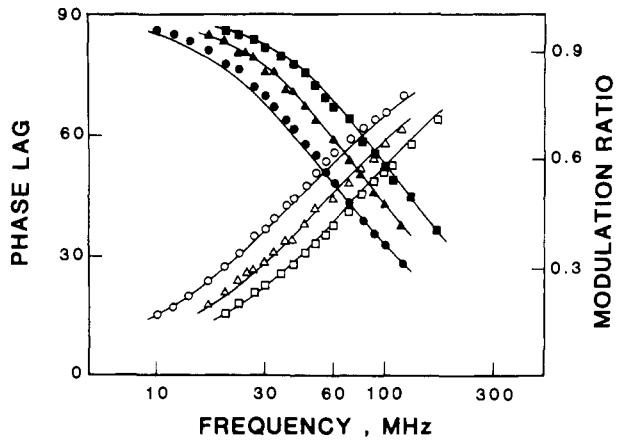

FIGURE 8: Simultaneous fit of phase/modulation for Ca^{2+}-loaded parvalbumin at acrylamide concentrations of 0 (○, ●), 0.46 M (△, ▲), and 1.06 M (□, ■). Data and fits for the other three acrylamide concentrations in Table III are not shown for simplicity. The global fit is for a Lorentzian distribution model, with the three parameters τ center = 3.4 ns, width = 1.7 ns, and $k_q = 0.18 \times 10^9$ M^{-1} s^{-1}.

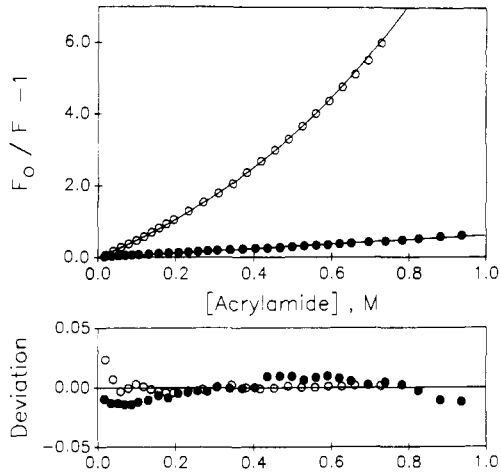

FIGURE 9: Stern–Volmer plots for the acrylamide quenching of the steady-state intensity of Ca^{2+}-loaded (●) and Ca^{2+}-depleted (○) protein. The fits shown are for the parameters given in Tables V and VI (type I for Ca^{2+}-loaded protein and type II for Ca^{2+}-depleted protein). The bottom shows the deviation ($F_{calcd} - F_{exp}$) patterns for the fits.

As the number of fitting parameters increases from 1 to 5, a better fit is achieved, as indicated by the lower χ^2 values. However, some of the fitting parameters are unreasonable. For example, the 1.4–2.5% contribution from a K_2 of 44.3–48.1, in fits III and IV for the Ca^{2+}-loaded protein, is larger than possible for diffusional controlled quenching.

As an alternative, we have considered a model in which there is a distribution of dynamic quenching constants, similar to the model for a distribution of lifetimes. If the latter model is a more realistic interpretation of lifetime data, then it follows, since $K = k_q\tau_o$, that there will be a distribution of quenching constants. The algorithm is described under Experimental Procedures. The solid curve in Figure 10A and the pseudo-Lorentzian distribution in Figure 10B illustrate the best fit obtained with such a model for the acrylamide quenching of the Ca^{2+}-loaded form of parvalbumin. We note that a distribution of lifetimes will result in a Stern–Volmer plot that is slightly downward curving. A static component was also included in the fit in Figure 8B.

We also performed limited studies of the quenching by KI of the fluorescence of the two forms of the proteins. In both cases, the Stern–Volmer plots were linear, and the K values were calculated to be 0.14 M^{-1} for Ca^{2+}-loaded parvalbumin and 2.60 M^{-1} for Ca^{2+}-depleted parvalbumin.

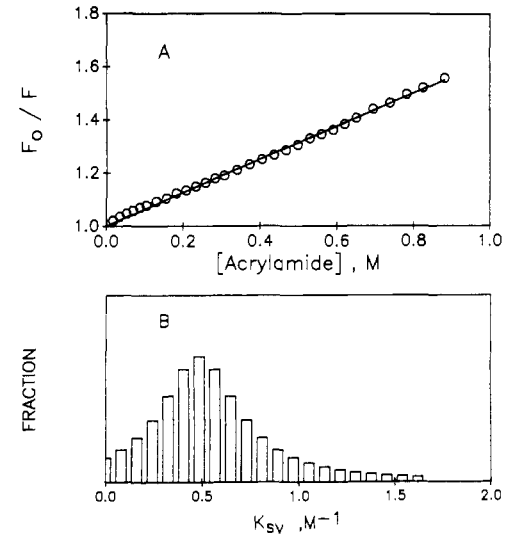

FIGURE 10: (A) Fit of the Lorentzian distribution model to steady-state quenching data for Ca^{2+}-loaded parvalbumin. (B) Distribution of K_{SV} values. See Table IV for parameters.

Discussion

Cod parvalbumin is another example of a protein that shows a nonexponential fluorescence decay, even when highly purified. The departure from exponentiality is not great, particularly for the Ca^{2+}-loaded form. In fact, Castelli et al. (1988) have recently reported that the decay of the homologous whiting parvalbumin is a monoexponential, making it one of the very few proteins to show such a simple fluorescence decay. We can only speculate that the difference in the position of the single Trp residues (position 109 for the cod protein vs position 102 for the whiting protein) or the differences in pH and salt concentration used in the two studies can explain the different results.

The physical basis for the complex kinetic decay, which we see for both Ca^{2+}-loaded and -depleted cod parvalbumin, is a question of general importance. A description in terms of two discrete decay times is possible, but so is a description in terms of a continuous distribution of decay times. Permyakov et al. (1985), in their previous study with whiting parvalbumin, proposed that there exist two conformational states of the protein, a folded conformer and a partially unfolded (relaxed) conformer. The key question is whether there exist two distinct conformers or a quasi-continuous distribution of conformers. From individual fluorescence decay measurement alone, it may not be possible to make the distinction, at least with the data that we can presently obtain (Alcala et al., 1987a; Lakowicz et al., 1987a; James et al., 1985; Wagner et al., 1987). Phase-resolved spectra are obtained for the two lifetime components (see Figure 6), but this does not mean that there are in fact two discrete fluorescing states. If you tell the phase fluorometer that there are only two decay times, it will display only two phase-resolved spectra.

To try to distinguish between a discrete (two-component) fit and a quasi-continuous distribution fit, we present here studies of the temperature dependence and quencher concentration dependence of frequency domain data for parvalbumin. Our strategy is to see if the lifetime fits (either discrete or distribution fits) will be consistent over both these T and [Q] data sets. We employ the powerful method of global nonlinear least-squares analysis to test the linkage of the T and [Q] data sets, via an Arrhenius or Stern–Volmer relationship. Also, we have studied the steady-state quenching of the fluorescence

of parvalbumin to see if such data are consistent with the T and [Q] frequency domain fits.

Below we will discuss these studies and the insights that they provide regarding the choice between the discrete lifetime model and the continuous distribution lifetime model.

Temperature Dependence Studies. For the Ca^{2+}-loaded protein (Table I; Figures 4 and 5), we see adequate fits with both the discrete (two-component) and distribution models. The fact that the χ^2 for the global distribution fit (three parameters) is lower than that for the two-component/α_i-linked fit (five parameters) indicates preference for the former model. When the α_i are allowed to vary at each temperature (12 parameters), the fit is superior, but the α_i are found to change randomly with change in temperature. The distribution fit is thus favored for fitting the temperature dependence data for the Ca^{2+}-loaded protein.

For the Ca^{+}-depleted protein, it is difficult to favor the distribution fit. The decay kinetics deviate more from monoexponentiality than for the Ca^{2+}-loaded case, and the two discrete component fits seem superior to the single, broad distribution fits. With the global two-component/α_i-varied fit, the α_i are not constant at all temperatures. In fact the fitted α_1 drop gradually with increasing temperature. Such a drop may reflect a temperature-dependent shift in the equilibrium between two conformations of the protein. It is not unreasonable that removal of Ca^{2+} from parvalbumin will result in different, interconvertible conformational states. In fact, Filimonov et al. (1978) and Permyakov et al. (1987) have presented scanning calorimetric and fluorescence data which are consistent with the existence of two-state thermal unfolding of Ca^{2+}-depleted carp and cod parvalbumin with $T_m \approx 32$ °C.

We have limited our analysis to two discrete components (and/or one distribution). It is likely, of course, that three or more components (either discrete or distributed) are needed to adequately fit the decay kinetic due to the existence of multiple conformational states in the Ca^{2+}-depleted protein. We have not attempted to fit a three-component model to our data.

Regardless, the temperature dependence data seem to favor the discrete two-component fit over the distribution fit for the Ca^{2+}-depleted protein.

Acrylamide Quenching, Frequency Domain Studies. For the Ca^{2+}-loaded protein (Table III; Figure 7, top), the distribution fit again seems most adequate for describing the quenching data. The Stern–Volmer plot in Figure 7 seems to support the two-component fit, since the individual τ_i appear to follow the Stern–Volmer relationship with reasonable k_q values. But these discrete fits call for the α_1 to decrease with increasing [Q]. This would only be possible if there were a selective, static quenching of the long-lifetime component. The distribution fit, on the other hand, provides a fit with only a slightly larger χ^2, with much fewer fitting parameters, with a lifetime and width similar to those obtained for the temperature dependence distribution fit, and with a reasonable k_q. For the Ca^{2+}-depleted protein the individual Stern–Volmer plots for the two-components fits have a very unsatisfactory appearance (Figure 7, bottom). When we performed the global two-component/α_i-varied analysis, in which Stern–Volmer behavior is required for the individual components, the α_1 is found to decrease markedly with increasing [Q]. Again this could reflect selective static quenching of the long-lifetime component by acrylamide, which is a possibility that is difficult to rationalize. When the α_i are linked, the fit is nearly as good as when the α_i are allowed to vary, but the fitted τ_i and α_i are not in very good agreement with the similar α_i-linked fit for the temperature data. Likewise, the global distribution fit for the [Q] data is adequate, but the central lifetime is significantly lower than that found for the similar global fit for the temperature data. So, as with the temperature dependence fits, it is not clear which model (two discrete components or distribution) is best to describe the data for the Ca^{2+}-depleted protein, and this probably is due to the fact that an even more complex model (i.e., three components) is necessary.

We note that, for all of the frequency domain quenching studies, we assume that the simple Stern–Volmer relationship holds. Recently, Lakowicz and co-workers (Lakowicz et al., 1987b,c) have shown that the transient term for diffusional quenching reactions can produce a significant contribution to decay data as quencher is added and that this transient effect can thus complicate the fluorescence decay order (i.e., make an otherwise exponential decay become nonexponential in the presence of quencher). We have not included this transient term in our analysis at this time. It may be useful to do so in the future.

Acrylamide Quenching, Steady-State Studies. In principle, steady-state fluorescence quenching data should be described by some of the same fitting parameters as are required for lifetime data. The dynamic quenching constants, K_i, are equal to $k_{q,i}\tau_{o,i}$, and the fractional intensity f_i associated with each accessible component is related to the preexponential (α_i) parameters as $f_i = \alpha_i\tau_{oi}/\sum\alpha_i\tau_{oi}$. Therefore, there should be consistency in the fits to steady-state and lifetime fits for an acceptable model. Of course static quenching, described by static quenching constants V_i, can complicate steady-state analyses. Nevertheless, a valid model should be able to describe both lifetime data and steady-state quenching data. An example in which steady-state data has confirmed lifetime fits is liver alcohol dehydrogenase. The decay kinetics of this enzyme have been fitted to a biexponential, with a long lifetime of ~7 ns and a short lifetime of ~3.5 ns [Ross et al., 1981b; Eftink & Hagaman, 1986; see, however, the report by Demmer et al. (1987) that the long-lifetime component may be biexponential]. Steady-state quenching studies with iodide and acrylamide are consistent with this two-component fit and further show that the short-lifetime component represents an inaccessible Trp residue, Trp-314.

Likewise, we consider whether steady-state acrylamide quenching studies with parvalbumin (Tables V and VI; Figures 9 and 10) are consistent with the two-component or distribution fits for the decay kinetics.

For the Ca^{2+}-loaded protein, the Stern–Volmer plot is nearly linear (Figures 9 and 10). As indicated by the fits in Table V, inclusion of static quenching constants and a second component results in a modest improvement in the χ^2. For fits III and IV, unreasonably large K_2 values (which also have a very small f_2) are obtained, and so such fits must not be given much credence over the simple, one-component fit I. The K for fit I is 0.62 M^{-1}. From our frequency domain quenching studies in Table III, it turns out that, for the global two-component fits, the product $k_{q,i}\tau_{o,i}$ is about 0.6 M^{-1} for each component. Or, looking at the individual (short and long lifetime) Stern–Volmer plots in Figure 7 (top), the $K_{sv,i}$ are in the range of 0.5–0.8 M^{-1}. Therefore, there is consistency between the frequency domain and steady-state fits.

The lifetime distribution fit is also consistent with the steady-state quenching data for the Ca^{2+}-loaded protein. We have fitted the steady-state quenching data with a model in which there is a Lorentzian distribution of K_i values. This situation, of course, could exist if there is a similar distribution

of fluorescence lifetimes, since $K = k_q\tau_o$. (It is also possible that the k_q values may be distributed, rather than being a discrete value.) As shown in Table V and Figure 10, an adequate fit can be achieved with a distribution of quenching constants centered at 0.42 M^{-1} and with a width of 0.63 M^{-1}. A small static component of 0.12 M^{-1} was also included to improve the fit. This distribution fit cannot be claimed to be better than the simpler fits to a single component (fits I and II in Table V). In fact the χ^2 are comparable. However, the distribution fit can certainly be said to be consistent with the steady-state data.

For the Ca^{2+}-depleted protein, the strong static quenching component makes it difficult to try to compare fits to the frequency domain data. In Table VI we see that either a one-component with static (fit II) or a two-component with static (fit IV) quenching model is adequate to describe the steady-state data. The dynamic quenching constants of 4.9 M^{-1} for fit II and 2.1 and 5.7 M^{-1} for fit IV are in reasonable agreement with the global two-component (α_f-linked) fit of the frequency domain quenching data in Table IV, which yielded individual $k_{q,i}\tau_{o,i}$ of 4.5 M^{-1} and 8.2 M^{-1}. The masking effect of the static quenching term makes further comparison difficult, and we have not attempted to fit a distribution of quenching constants to the steady-state data for Ca^{2+}-depleted parvalbumin.

Summary

The question of whether the fluorescence of a single Trp residue in a protein should be described by two or more discrete components or whether it should be described in terms of a pseudo-continuous distribution (of Lorentzian or other shape) of components is one that is very difficult to answer. Even for systems as simple as tryptophan in water, the question applies (Wagner et al., 1987; Lakowicz et al., 1987a). It is very difficult to decide between these two models on the basis of the goodness of fits to data. Data of very high quality are needed to even attempt to distinguish between such models by analysis of time or frequency domain data alone (James & Ware, 1985; Alcala et al., 1987a; Lakowicz et al., 1987a).

Here we have employed the strategy of (1) collecting temperature dependence and [Q] dependence frequency domain data, along with steady-state quenching data, and (2) trying to determine whether the different models (two discrete vs Lorentzian distribution) are internally consistent with all data sets obtained for the fluorescence of the single Trp residue in cod parvalbumin. For the Ca^{2+}-loaded form of this protein, the distribution model seems to be more consistent with all the data sets. The single Trp residue is relatively buried to the quenchers acrylamide and iodide (k_q of 0.2×10^9 M^{-1} s^{-1} and 0.04×10^9 M^{-1} s^{-1}, respectively), and we speculate that librational and rotational fluctuations of the Trp side chain and that of surrounding amino acid residues give rise to the distribution of decay times.

For the Ca^{2+}-depleted form of parvalbumin, it is not clear that either the two-state or distribution model is adequate, and a more complex model may be necessary to describe all the data. The quenching studies show the Trp residue to be much more solvent exposed ($k_q \approx 2 \times 10^9$ and 1×10^9 M^{-1} s^{-1} for acrylamide and iodide, respectively) after removal of Ca^{2+}. The protein is expected to have lost much of its structural coherence, and at least two conformational states are likely to exist in equilibrium in the temperature range of 2–35 °C.

Acknowledgments

We thank Dr. Joseph M. Beechem, University of Illinois, for providing us with a copy of his program GLOBAL.

Registry No. Acrylamide, 79-06-1.

References

Albery, W. J., Bartlett, P. N., Wilde, C. P., & Darwent, J. R. (1985) *J. Am. Chem. Soc. 107*, 1854–1858.

Alcala, J. R., Gratton, E., & Prendergast, F. G. (1987a) *Biophys. J. 51*, 587–596.

Alcala, J. R., Gratton, E., & Prendergast, F. G. (1987b) *Biophys. J. 51*, 597–604.

Alcala, J. R., Gratton, E., & Prendergast, F. G. (1987c) *Biophys. J. 51*, 925–936.

Beddard, G. S., Fleming, G. R., Portor, G., & Robbins, R. J. (1980) *Philos. Trans. R. Soc. London, A 298*, 321–334.

Beechem, J. M., & Brand, L. (1985) *Annu. Rev. Biochem. 54*, 43–71.

Beechem, J. M., & Gratton, E. (1988) in *Time Resolved Laser Spectroscopy in Biochemistry, Proc. SPIE 909*, 70–81.

Beechem, J. M., Knutson, J. R., Ross, J. B. A., Turner, B. W., & Brand, L. (1983) *Biochemistry 22*, 6054–6058.

Beechem, J. M., Ameloot, M., Knutson, J. R., & Brand, L. (1988) in *Fluorescence Spectroscopy: Theory and Application* (Lakowicz, J. R., Ed.) Plenum (in press).

Blum, H. E., Lehky, P., Kohler, L., Stein, E. A., & Fischer, E. H. (1977) *J. Biol. Chem. 252*, 2834–2838.

Brochon, J. C., Wahl, P., & Auchet, J. C. (1974) *Eur. J. Biochem. 41*, 557–583.

Castelli, F., White, H. D., & Forster, L. S. (1988) *Biochemistry 27*, 3366–3372.

Chen, L. S., Longworth, J. W., & Fleming, G. R. (1987) *Biophys. J. 51*, 865–873.

Closset, J. I., & Gerday, C. (1976) *Comp. Biochem. Physiol. B: Comp. Biochem. 55B*, 537–542.

Demmer, D. R., James, D. R., Steer, D. P., & Verral, R. E. (1987) *Photochem. Photobiol. 45*, 39–48.

Eftink, M. R., & Ghiron, C. A. (1976) *Biochemistry 15*, 672–680.

Eftink, M. R., & Hagaman, K. A. (1985) *Biophys. Chem. 22*, 173–180.

Eftink, M. R., & Hagaman, K. A. (1986) *Biochemistry 25*, 6631–6637.

Eftink, M. R., & Ghiron, C. A. (1987) *Biophys. J. 52*, 467–473.

Eftink, M. R., Ghiron, C. A., & Wasylewski, Z. (1987) *Biochemistry 26*, 8338–8346.

Filimonov, V. V., Pfeil, W., Tsalkova, T. N., & Privalov, P. L. (1978) *Biophys. Chem. 8*, 117–122.

Francois, J.-M., Sedarous, Gerday, C., Gratton, E., & Prendergast, F. G. (1987) *Biophys. J. 51*, 276a.

Gratton, E., & Jameson, D. M. (1985) *Anal. Chem. 57*, 1694–1697.

Gratton, E., Limkeman, M., Lakowicz, J. R., Maliwal, B. P., Cherek, H., & Laczko, G. (1984) *Biophys. J. 46*, 479–486.

Grinvald, A., & Steinberg, I. Z. (1976) *Biochim. Biophys. Acta 427*, 663–678.

Haiech, J., Derancourt, J., Pechere, J.-F., & Demaille, J. G. (1979) *Biochemistry 18*, 2752–2758.

Horrocks, W. DeW., Jr., & Collier, W. E. (1981) *J. Am. Chem. Soc. 103*, 2856–2861.

Iio, T., & Hoshihara, Y. (1984) *J. Biochem. (Tokyo) 96*, 321–328.

James, D. R., & Ware, W. R. (1985) *Chem. Phys. Lett. 120*, 455–459.

James, D. R., Liu, Y.-S., deMayo, P., & Ware, W. R. (1985) *Chem. Phys. Lett. 120*, 460–465.

Kretsinger, R. H. (1980) *CRC Crit. Rev. Biochem. 10*, 119–174.

Lakowicz, J. R., Laczko, G., Cherek, H., Gratton, E., & Limkeman, M. (1984) *Biophys. J. 46*, 463-477.
Lakowicz, J. R., Laczko, G., Gryczynski, I., & Cherek, H. (1986) *J. Biol. Chem. 261*, 2240-2245.
Lakowicz, J. R., Cherek, H., Gryczynski, I., Joshi, N., & Johnson, M. L. (1987a) *Biophys. Chem. 28*, 35-50.
Lakowicz, J. R., Johnson, M. L., Gryczynski, I., Joshi, N., & Laczko, G. (1987b) *J. Phys. Chem. 91*, 3277-3285.
Lakowicz, J. R., Joshi, N. B., Johnson, M. L., Szmacinski, H., & Gryczynski, I. (1987c) *J. Biol. Chem. 262*, 10907-10910.
Ludescher, R. D., Volwerk, J. J., de Haas, G. H., & Hudson, B. S. (1985) *Biochemistry 24*, 7240-7249.
Ogawa, Y., & Tanokura, M. (1986) *J. Biochem. (Tokyo) 99*, 73-80.
Permyakov, E. A., Yarmolenko, V. V., Emelyanenko, V. I., Burstein, E. A., Closset, J., & Gerday, Ch. (1980) *Eur. J. Biochem. 109*, 307-315.
Permyakov, E. A., Ostrovsky, A. V., Burstein, E. A., Pleshanov, P. G., & Gerday, Ch. (1985) *Arch. Biochem. Biophys. 240*, 781-792.
Permyakov, E. A., Ostrovsky, A. V., & Kalinichenko, L. P. (1987) *Biophys. Chem. 28*, 225-233.
Petrich, J. W., Chang, M. C., McDonald, D. B., & Fleming, G. R. (1983) *J. Am. Chem. Soc. 105*, 3824-3832.
Petrich, J. W., Longworth, J. W., & Fleming, G. R. (1987) *Biochemistry 26*, 2711-2722.
Rayner, D. M., & Szabo, A. G. (1978) *Can. J. Chem. 56*, 743-745.
Ross, J. B. A., Rousslang, K. W., & Brand, L. (1981a) *Biochemistry 20*, 4361-4368.
Ross, J. B. A., Schmidt, C. J., & Brand, L. (1981b) *Biochemistry 20*, 4369-4377.
Stryjewski, W., & Wasylewski, Z. (1986) *Eur. J. Biochem. 158*, 547-553.
Szabo, A. G., & Rayner, D. M. (1980) *J. Am. Chem. Soc. 102*, 554-563.
Szabo, A. G., Stepanik, T. M., Wayner, D. M., & Young N. M. (1983) *Biophys. J. 41*, 233-244.
Wagner, B. D., James, D. R., & Ware, W. R. (1987) *Chem. Phys. Lett. 138*, 181-184.

Amino Acid Sequence of a Mouse Mucosal Mast Cell Protease†

Hai Le Trong,‡ George F. J. Newlands,§ Hugh R. P. Miller,§ Harry Charbonneau,‡ Hans Neurath,‡ and Richard G. Woodbury*,‡

Department of Biochemistry, SJ-70, University of Washington, Seattle, Washington 98195, and Moredun Research Institute, 408 Gilmerton Road, Edinburgh EH17 7JH, United Kingdom

Received July 28, 1988; Revised Manuscript Received September 23, 1988

ABSTRACT: The amino acid sequence has been determined of a mouse mucosal mast cell protease isolated from the small intestines of mice infected with *Trichinella spiralis*. The active protease contains 226 residues. Those corresponding to the catalytic triad of the active site of mammalian serine proteases (His-57, Asp-102, and Ser-195 in chymotrypsin) occur in identical positions. A computer search for homology indicates 74.3% and 74.1% sequence identity of the mouse mast cell protease compared to those of rat mast cell proteases I and II (RMCP I and II), respectively. The six half-cystine residues in the mouse mast cell protease are located in the same positions as in the rat mast cell proteases, cathepsin G, and the lymphocyte proteases, suggesting that they all have identical disulfide bond arrangements. At physiological pH, the mouse and rat mucosal mast cell proteases have net charges of +3 and +4, respectively, as compared to +18 for the protease (RMCP I) from rat connective tissue mast cells. This observation is consistent with the difference in solubility between the mucosal and connective tissue mast cell proteases when the enzymes are extracted from their granules under physiological conditions.

The presence of high levels of proteolytic enzymes in basophilic secretion granules is a characteristic feature of mast cells. Benditt and Arase (1959) first detected in rat mast cells a protease with chymotrypsin-like specificity. Later, a second similar, yet distinct, protease was found in an unusual subtype of rat mast cells known as "atypical" or mucosal mast cells. They differed in histochemical properties from those of the peritoneal type and were exclusively localized in mucosal tissues of normal rats (Woodbury et al., 1978a). The protease from peritoneal mast cells is referred to as rat mast cell protease I (RMCP I)[1] and that from mucosal mast cells as RMCP II (Woodbury & Neurath, 1978). More recently, proteases resembling in substrate specificities and other properties those of rat peritoneal mast cells have been isolated from dog and human mast cells (Schechter et al., 1983; Powers et al., 1985). Additionally, proteases with trypsin-like or carboxypeptidase A like activity have been reported to be present in peritoneal rat mast cells (Everitt & Neurath, 1980; Kido et al., 1985; Serafin et al., 1987).

† This work was supported in part by grants from the National Institutes of Health (HL36114 and GM15731).
* Address correspondence to this author.
‡ University of Washington.
§ Moredun Research Institute.

[1] Abbreviations: MMMCP, mouse mucosal mast cell protease; RMCP I, rat mast cell protease I; RMCP II, rat mast cell protease II; CM, *S*-(carboxymethyl); HPLC, high-performance liquid chromatography; Tris-HCl, tris(hydroxymethyl)aminomethane hydrochloride; EDTA, ethylenediaminetetraacetic acid.

0006-2960/89/0428-0391$01.50/0